Glycosylation Heterogeneity of Hyperglycosylated Recombinant Human Interferon-β (rhIFN-β)

Kyoung Song[1], Dae Bong Moon[2], Na Young Kim[3], and Young Kee Shin[4]

[1]LOGONE Bio Convergence Research Foundation
[2]Binex Co.,Ltd.
[3]ABION Inc.
[4]Seoul National University

April 28, 2020

Abstract

We previously developed a biobetter version of rhIFN-β (R27T) that possesses an additional glycosylation site compared with rhIFN-β 1a. Herein, we characterized N-glycosylation heterogeneity of R27T. N-glycan site occupancy manifested as distinct differences in size. The analysis of complex carbohydrate moieties of R27T involved the common biopharmaceutical glycosylation critical quality attributes like core fucosylation, antennary composition, sialylation, lactosamine extensions, linkages, and overall glycan profiles using weak anion exchange and hydrophilic interaction HPLC with 2-aminobenzoic acid-labeled N-glycans. The double-glycosylated form accounted for approx. 94% R27T, while the single-glycosylated form accounted for 6% R27T. N-glycans consisted of a mixture of bi-, tri-, and tetra-antennary glycans, some with lactosamine extensions, but neither outer arm fucose nor α-galactose was detected. Sialic acid major variants, N-acetyl- and N-glycolyl-neuraminic acid were more abundant in R27T than in Rebif. The major N-glycan, accounting for 42% of total N-glycans, had a di-sialylated, core-fucosylated biantennary structure.

Introduction

Several immunomodulatory treatments have been approved by the US Food and Drug Administration (FDA) and European Medicines Agency (EMA) for relapsing-remitting forms of multiple sclerosis (RRMS) (Chen, Wu, & Watson, 2018; Diebold & Derfuss, 2016; Goodin et al., 2002; Madsen, 2017). Among them, recombinant human interferon-β (rhIFN-β) has long been used as an effective first therapeutic intervention and disease-modifying therapy (DMT) for RRMS (Borden et al., 2007; Kappos et al., 2007; Kappos et al., 2006). Though almost three decades have passed since the introduction of rhIFN-β therapies, they remain important for the management of MS due to their good long-term safety profile and cost-efficacy (Castro-Borrero et al., 2012; Dumitrescu, Constantinescu, & Tanasescu, 2018; Gasperini & Ruggieri, 2011). However, there are direct and indirect limitations for clinical use including the need for frequent injections, and high immunogenicity and aggregation propensity, the latter of which is responsible for the therapeutic effect of the protein (Grossberg, Oger, Grossberg, Gehchan, & Klein, 2011; Hartung, Munschauer, & Schellekens, 2005; van Beers, Jiskoot, & Schellekens, 2010). To address these issues, in our previous study, an additional single-glycosylation site was introduced at amino acid 25 in rhIFN-β 1a, resulting in R27T in which Arg at position 27 is mutated to Thr (Song et al., 2014). The additional glycosylation site increases the half-life and *in vitro* biological activity, as well as thermostability, allowing less frequent dosing (Lee et al., 2018; Song et al., 2014).

As observed for R27T, glyco-engineering of therapeutic proteins can enhance *in vivo* activities by improving pharmacokinetic properties, solubility, thermal stability, and protease resistance, and reducing the immuno-

genicity, all of which may improve clinical outcomes (Ghaderi, Zhang, Hurtado-Ziola, & Varki, 2012; Hossler, Khattak, & Li, 2009; Sareneva, Pirhonen, Cantell, & Julkunen, 1995; Sola & Griebenow, 2010; Walsh & Jefferis, 2006; Wright & Morrison, 1997). However, despite its importance, it is very difficult to accurately determine the influence of glycosylation on glycoproteins due to its inherent complexity. Potential glycosylation sites such as Asn residues within Asn-X-Ser/Thr consensus sequences are not always occupied by oligosaccharides in mammalian cells because a consensus sequence alone is essential but not sufficient for N-linked protein glycosylation, resulting in site occupancy heterogeneity (macroheterogeneity) (Jenkins, Parekh, & James, 1996; Zhang, Li, Lu, & Liu, 2017). In addition, the composition of attached oligosaccharides can also vary considerably, although a core pentasaccharide unit (Man3GlcNAc2) is typically linked to an asparagine (Asn) residue via a chitobiose (GlcNAc2) (Barry et al., 2013). The glycan structure can be highly variable in terms of antennary structure, monosaccharide composition, and sialylation depending on host cell type, cell culture, and manufacturing conditions (Becerra-Arteaga & Shuler, 2007; Joosten & Shuler, 2003; Nam, Zhang, Ermonval, Linhardt, & Sharfstein, 2008; Wurm, 2004). This results in inherent structural complexity and variability (microheterogeneity) (Zhang et al., 2017). Since the complexity of glycosylation heterogeneity makes it difficult to understand structure-function relationships, it is imperative to characterize glycosylation variability. Herein, we performed a comprehensive characterization of the main R27T glycoforms. Glycosylation analysis can identify glycosylation parameters that may influence drug safety and efficacy profiles via critical quality attributes (CQAs). In the present study, we investigated common biopharmaceutical glycosylation CQAs including site occupancy heterogeneity, core fucosylation, antennary composition, sialylation, lactosamine extensions, linkages, and overall glycan profiles of R27T glycan.

Materials and Methods

SDS-PAGE and Microchip Analysis

Each sample preparation was described in the Experimental section in the Supporting Information. Samples (0.8 mg/mL, 30 μL) were denatured at 100°C for 3 min after mixing with reducing buffers. Separation took place at 100 V for 30 min within the stacking gel, and 130 V for 2 h within the 12% TRIS-glycine mini gel. Coomassie Blue staining was used for protein visualization, and quantitative microchip analysis based on protein size was performed using a Protein 230 kit (Agilent Technologies, Waldbronn, Germany) following the manufacturer's protocol on an Agilent 2100 Bioanalyzer (Agilent Technologies).

IEF and cIEF Analysis

IEF was used to confirm the pI of proteins and was performed using a pH 3-10 IEF gel (Invitrogen, CA, USA) with 18 μg samples. Coomassie Blue staining was used for visualization. To quantitate each pI band, we performed cIEF using a neutral capillary (50 μm internal diameter; total length, 30.2 cm; effective length, 20 cm) on a PA800 plus CE instrument (Beckman Coulter, Brea, CA, USA). Samples (5 mg/mL, 10 μL) were prepared and mixed with 240 μL of master mix, and 200 μL was loaded onto the sample tray. UV detection was performed at 280 nm.

Determining Sialic Acid Content and Variation

Sialic Acid Release and Labeling Kit (Ludger) and Monosaccharide Release and Labeling Kit (Ludger) were used to analyze the sialic acid and galactose contents, respectively. The detailed information was described in the Experimental section in the Supporting Information. UPLC analysis was performed within 24 min of sample preparation on an Agilent 1290 Infinity II System equipped with a fluorescence detector (excitation = 373 nm, emission = 448 nm). A 5 μL sample was injected onto a LudgerSep uR2 column (LS-UR2-2.1×100 for sialic acid, LS-UR2-2.1×50 for galactose). Each sample was applied after equilibrating the column with acetonitrile:methanol:water (9:7:84%) at 0.25 mL/min (for sialic acid) or BPT solvent at 30°C.

Determining the Antennary Structure by Exoglycosidase Sequencing

The 2-aminobenzoic acid (2-AB)-labeled glycans derived from R27T were incubated overnight at 37°C with various exoglycosidase enzymes in 50 mM sodium acetate pH 5.5. The detailed information for N-glycan

release and labeling was described in the Experimental section in the Supporting Information. Enzymes were removed by a protein-binding membrane, and samples were analyzed by HILIC-HPLC using an LSN2-40m-Nlink-35%_G100 and a LudgerSep-N2 column (LS-N24.6×150) on a Waters 2795 HPLC instrument linked to a 2475 fluorescence detector controlled by Empower software version 2, build 2154. The detailed HPLC condition was described in the Experimental section in the Supporting Information. 2-AB-labeled glucose homopolymer (Ludger product CAB-GHP-30, 2-AB glucose homopolymer ladder) was used as a system suitability standard as well as an external calibration standard for GU allocation (the system is deemed to be within specifications if the peak width at half height for GU10 is less than 0.4 min).

Determining N-glycan Structures by WAX/HILIC-HPLC with Fluorescence Labeling of Glycans

The 2-AB-labeled glycans derived from R27T were separated using a LudgerSep-C3 WAX-HPLC column with manual fraction collection of the separated peaks. Collected fractions were desalted by evaporation of the HPLC buffer in a centrifugal evaporator followed by the addition of 1 mL aliquots of water to each fraction and subsequent centrifugal evaporation of the water. This process was repeated until no salt deposit was visible. Half of each fraction was analyzed directly by LudgerSep-N2 HILIC-HPLC, and the remaining half was digested with sialidase then analyzed by LudgerSep-N2 HILIC-HPLC. For sialidase digestion, aliquots of 2-AB-labeled glycan fractions were incubated overnight at 37°C with Sialidase (E-S001; QABio) (a368S; specific for a2-3, -6, -8, and -9 sialic acids) in 50 mM sodium acetate pH 5.5. Enzyme was removed using a protein-binding membrane before analysis by LudgerSep-N2 HILIC-HPLC.

Determining N-glycan Structures by HILIC-MS

Aliquots (1 μL) of the unlabeled portion of N-glycans released from samples were taken for permethylation analysis along with negative and positive controls (buffer, water, and fetuin). Unlabeled glycan samples were permethylated using methyl iodide in a dimethylsulfoxide (DMSO)/NaOH suspension for in-solution permethylation of glycans. Permethylated glycans were obtained from solution by extracting with chloroform, and samples were run on a Shimadzu-Biotech Resonance MALDI mass spectrometer using 10 mg/mL 2,5-dihydroxybenzoic acid (DHB) in acetonitrile as the matrix.

Results and Discussion

N-glycosylation Site Occupancy Heterogeneity

We analyzed three batches of R27T purification products and purification intermediates. We defined proteins separated by hydrophobicity over four column steps into main target (R27T) and intermediate (shoulder) peaks (Figure S1). Each peak was analyzed by SDS-PAGE and IEF with Rebif, a single-glycosylated rhIFN-β, as a reference (Figure 1A). The main R27T peaks revealed a protein of ˜25-26 kDa with an isoelectric point (pI) of ˜5.3-6.9 and a smear pI of 7.5, 8.0 and 8.3 on IEF gels, while Rebif ran as a 22.5 kDa product with major pI values of 8.0 and 8.3. Intermediate peaks separated from major peaks yielded a broad medium-sized band that ran between the R27T and Rebif bands, and its pI bands were more basic than those of R27T, and some were within the main pI range of Rebif, indicating a mixture of single- and double-glycosylated proteins. We attempted to quantitate species with one or two glycosylation sites to analyze glycosylation site occupancy heterogeneity. We used a microchip assay and capillary IEF (cIEF) to separate and quantitate species based on size and pI differences (Figure 1B, 1C). We were able to correlate the size with glycosylation occupancy, although there was considerable size variation (˜15.2 kDa for no glycosylation, 21.9-34.8 kDa for one glycosylation, and 41.6-45.7 kDa for two glycosylation, Table S1) compared with qualitative analysis due to limitations of the capillary analysis methods with glycoproteins (Engel et al., 2015). There were also clear differences in pI (˜7.19-7.97 for one glycosylation and 5.67-7.09 for two glycosylation). Based on size differences, we found that R27T was made up of 94% of the double glycosylated form and 6% of the single-glycosylated form (Figure 1B). For the R27T intermediate, the ratio was 5%, 77%, and 18% non-glycosylated, single-glycosylated, and double-glycosylated, respectively. By contrast, the Rebif reference protein displayed 100% single-glycosylated form. These results were supported by cIEF, although there was a slight difference in ratios (94.1% double-glycosylation and 1.9% single-glycosylation for R27T, and 84.5% single-glycosylation

and 12.2% double-glycosylation for the R27T intermediate), because of more direct effect of number of sialic acid rather than number of glycan chain. (Figure 1C). The inclusion of the 6% single-glycosylated form as a macroheterogeneity with the 94% double-glycosylation form of R27T did not have a significant influence on the specific activity as discussed in our previous study (Song et al., 2014). Thus, the presence of 6% single-glycosylated R27T could be considered a control factor for more homogeneous molecular entity and an example of macroheterogeneity, but such products would not fail to meet the quality criteria.

Sialic Acid Content and Variation

Since sialic acids are terminal, negatively charged components that can determine the serum half-life and influence immunogenicity and biological activity, they are typically considered glycosylation CQAs. The abundance and terminal capping ratio of sialic acids on galactose are very important because they impact the function and biological half-life of biopharmaceuticals, since neutral glycans without sialic acid are cleared by asialoglycoprotein receptors in the liver (Achord, Brot, & Sly, 1977; Dobryszycka & Kukral, 1970; Morell, Irvine, Sternlieb, Scheinberg, & Ashwell, 1968).

Overall charge profiles for R27T was shown according to the number of sialic acids (Figure S2). The 2S component was the most abundant (35.6%) followed by 1S (26.1%), 3S (21.7%), and 4S (16.6%). The absolute quantitation of sialic acid residues of R27T was also measured as the molar ratio of sialic acid per R27T molecule (Table 1). The sialic acid content of R27T (2.81 mol/mol protein) was, as expected, much greater (3-fold) than that of Rebif (0.77 mol/mol protein), and the value was consistent with that in our previous study (Song et al., 2014). Sufficient sialylation can prolong the half-life, as demonstrated in our previous study (Song et al., 2014).Galactose monosaccharide analysis was performed to investigate the sialic acid capping ratio and evaluate the quality of R27T and Rebif (Table 1). The terminal sialic acid capping ratio on galactose was ˜0.28-0.31 for both R27T and Rebif samples.

Another important aspect of sialylation is variation, which mainly includes *N* -acetyl-neuraminic acid (Neu5Ac) and*N* -glycolyl-neuraminic acid (Neu5Gc). Since Neu5Gc cannot be synthesized in humans, it may be recognized as a foreign epitope with immunogenic potential(Ghaderi, Taylor, Padler-Karavani, Diaz, & Varki, 2010; Hokke et al., 1990). Numerous studies have illustrated the necessity to minimize the relative content of Neu5Gc sialic acids in glycoprotein biopharmaceuticals(Ghaderi et al., 2010). Both sialic acid major variants, Neu5Ac and Neu5Gc were more abundant in R27T samples (2.75, 0.06 mol/mol protein, respectively) than in Rebif (0.77 mol/mol protein, not detected) (Table 1). The relative Neu5Gc percentage of total sialylation for R27T was 2.1%, but this was not detected for Rebif. In Chinese hamster ovary (CHO) cells, ˜3% of sialic acids were identified as Neu5Gc for recombinant plasminogen activator, follicle-stimulating hormone (FSH), and erythropoietin (EPO)(Hokke et al., 1990). In addition, EPO containing 1% Neu5Gc induces a negligible immunogenic response, whereas EPO with ˜7% Neu5Gc elicits a clinically significant immunogenic response (Noguchi, Mukuria, Suzuki, & Naiki, 1995). However, due to differences in products, as well as dosage and frequency for clinical use, it is difficult to generalize criteria values for Neu5Gc content in biopharmaceutical products. Various factors can be conveniently used to minimize or maintain Neu5Gc levels below 1% during the manufacturing of R27T (Borys et al., 2010).

Antennary Structures based on Exoglycosidase Sequencing

Detailed structures including core fucosylation, antennary composition, lactosamine extensions, and linkages were identified by exoglycosidase sequencing. The results of HILIC-HPLC analysis revealed 22 peaks (Figure S3, Table S2). Exoglycosidase treatment facilitated more accurate analysis of the N-glycan antennary structure of R27T (Figure 2). A summary of the results of exoglycosidase sequencing of N-glycans is included in Table S3. Data from sialidase (a368S), fucosidase (a34F, a6F), and galactosidase (a36G, b4G) exoglycosidase digestion can be used to quantify different types of antennary structures present within samples. A combination of enzymes can determine structures down to the core A2, A3, A3', and A4 structures, for which the glucose unit (GU) values are documented (Table S3). Digestion with α-galactosidase (a36G) or α-3/4 fucosidase (a34F) generated identical chromatograms, indicating that neither outer arm fucose nor α-galactose moieties were present. Comparison of digestion with sialidase (a368S) alone and digestion with

sialidase (a368S) plus both fucosidases (a34F and a6F) revealed that most peaks moved by ˜0.4 GU units, in line with the loss of a core α1-6 fucose component. This means that core-fucosylated structures accounted for 94% of the total. A comparison of digestion with sialidase (a368S) plus fucosidases (a34F and a6F) and digestion with sialidase (a368S) plus fucosidases (a34F and a6F) plus beta-galactosidase (b4G) revealed the core antennary structures (A2, A3, A3', and A4) for some peaks. However, a number of peaks did not digest and reveal the core structures until *N* -acetylglucosaminidase (sph) was also added, presumably because they contained lactosamine extension, which can be added to any antennae, resulting in diverse isomeric structures. Biantennary structures were most abundant. The N-glycan of R27T consists of a mixture of bi- (42.5%), tri- (17.2), and tetra-antennary glycans (8.8%), some of which have lactosamine extensions (29.3%). Most glycans in R27T (˜94%) also have a core-fucosylated structure (Table 2). This could play a crucial role in stabilization of the R27T structure because the core fucose structure of the rhIFN-β carbohydrate may help to stabilize the rhIFN-β structure (Karpusas, Whitty, Runkel, & Hochman, 1998). In these structures, galactose α1-3 linked to β-galactose was not observed. This is also very important because the presence of α-galactose could lead to potential adverse reactions, immunogenic potential, and neutralization of the drug by anti-α-galactose antibodies (Eon-Duval, Broly, & Gleixner, 2012).

N-glycan Structure Determination

We performed glycan structure profiling of R27T. Herein, two strategies for comprehensive N-glycan profiling, fluorescence profiling by WAX/HILIC-HPLC, in which an HPLC database is publicly available (Campbell, Royle, Radcliffe, Dwek, & Rudd, 2008; Royle et al., 2008; Royle, Radcliffe, Dwek, & Rudd, 2006), and MALDI-MS, were employed in this study.

N-glycan Profiles based on AEX- and HILIC-HPLC

Since sialic acid is the most common CQA for biopharmaceutical products, it can be useful to separate N-glycans on the basis of charge by WAX-HPLC, enabling more accurate relative quantification of multi-sialylated structures. R27T glycans were separated on a WAX-HPLC column, and 17 peak fractions were collected (Figure S4A). Fractions were combined (F2+F3, F4+F5, and F7+F8) when peaks were not clearly separated. Each fraction containing zero (F1), one (F4+F5), two (F7+F8), three (F9), or four (F10-13) sialic acids was then analyzed by HILIC-HPLC (Figure S4B). Fractions 2, 3, 6, and 14-17 did not contain any glycans. Fractions containing charged glycans were then digested with sialidase and re-run on the HILIC-HPLC column (Figure 3). Structures were identified from the GU values in relation to neutral structures identified by exoglycosidase sequencing. Fraction 1 contained neutral glycans (biantennary structures A2G2 and FA2G2). Fraction 4+5 contained mono-sialylated, core-fucosylated bi-, tri-, and tetra-antennary (with zero, one, or two lactosamine repeats) glycans. Fraction 7+8 contained di-sialylated glycans, and both major peaks (GU 8.4 and 8.9) digested to FA2G2 at GU 7.5. α2-3-linked sialic acid adds less to the GU value than α2-6-linked sialic acid. Thus, we can conclude that the largest peak (GU 8.4) includes an α2-3-linked sialic acid while the second peak (GU 8.9) has an α2-6-linked sialic acid. A small proportion of triantennary glycans were also di-sialylated. Fraction 9 contained tri-sialylated, core-fucosylated bi-, tri-, and tetra-antennary glycans with zero, one, or two lactosamine repeats. Both forms of triantennary glycans were identified: A3G3, in which the third GlcNAc is β1-4-linked to the 3-linked mannose, and A3'G3, in which the third GlcNAc is β1-6-linked to the 6-linked mannose. There were also some tri-sialylated tetra-antennary glycans without core fucose. Fraction 10 contained tetra-sialylated, core-fucosylated tetra-antennary glycans with two or three lactosamine repeats. Fraction 11 contained tetra-sialylated, core-fucosylated tetra-antennary glycans with two lactosamine repeats. Both peaks digested to the same GU value after removal of sialic acids, suggesting that the second smaller peak contained glycans with α2-6-linked sialic acid(s). Fraction 12 contained tetra-sialylated, core-fucosylated tetra-antennary glycans with one lactosamine repeat, as well as tetra-sialylated tetra-antennary glycans with and without core fucose. Fraction 13 contained tetra-sialylated, core-fucosylated tetra-antennary glycans. All peaks digested to the same GU value after removal of sialic acids, suggesting that the smaller peaks contained glycans with α2-6-linked sialic acid(s). The lactosamine extension adds approximately the same value to the GU value as the addition of an extra antenna (both are Gal-GlcNAc).

A summary of the identified glycans matched to peaks for the whole pool is given in Table 3 and Figure S5. The GU values changed slightly over time (this is normal for sialylated glycans); hence peaks in fractions were matched to a profile of the whole undigested pool run at the same time. The major N-glycan, which accounts for ˜42% of total N-glycans, is a di-sialylated, core-fucosylated biantennary structure. However, R27T also exhibited considerable variability in its glycoprofile, with tri- and tetra-antennary glycans, as well as biantennary glycan forms being detected. Surprisingly, rhIFN-β containing a larger proportion of higher antennary glycoforms showed more sustained bioactivity over time (Mastrangeli et al., 2015). Indeed, in our previous study, R27T exhibited more prolonged signaling than the mono-glycosylated rhIFN-β, with altered receptor-binding kinetics (Lee et al., 2018). A larger portion of higher antennary components in R27T may therefore influence cellular signaling effects.

Identification of N-glycan structures using MALDI-MS

MALDI spectra from permethylated N-glycans were consistent with most glycans being core-fucosylated biantennary types (FA2G2; H5N4F1) with zero, one, or two sialic acids (Figure 4). Masses corresponding to core-fucosylated triantennary glycans (FA3G3; H6N5F1) with one, two, or three sialic acids were also detected. We also acquired positive control data from the N-glycan of fetuin, and no peaks were detected in the negative controls (data not shown). Annotation of R27T N-glycan structures revealed complex glycans with variable degrees of core fucosylation, galactosylation, and sialylation. The major di-sialylated, core-fucosylated biantennary structure was consistent with the 2-AB labeling HPLC results.

Conclusion

We found the glycosylation heterogeneity of hyperglycosylated recombinant human interferon-β (rhIFN-β), R27T. The glycosylation site occupancy showed approx. 94% double-glycosylated form R27T with 6% single-glycosylated R27T. Microheterogeneity of R27T N-glycans had a mixture of bi-, tri-, and tetra-antennary glycans, some with lactosamine extensions, but neither outer arm fucose nor α-galactose was detected. Sialic acid major variants, Neu5Ac and Neu5Gc were more abundant in R27T than in Rebif. The major N-glycan, accounting for ˜42% of total N-glycans, had a di-sialylated, core-fucosylated biantennary structure. These findings could assist the development of second-generation rhIFN-β products, and help us better understand glycosylation CQAs and their biological significance.

Acknowledgement

We would like to thank ABION Inc (Seoul, Republic of Korea) for providing R27T and Rebif as well as Tae Won Yun from the LOGONE Bio Convergence Research Foundation for help with illustrations

Conflict of interest statement

Kyoung Song and Young Kee Shin currently hold stock and Na Young Kim hold stock options in ABION Inc.

Funding

N.A.

Authorship

Kyoung Song, Na Young Kim designed the study. Kyoung Song and Young Kee Shin contributed to the conceptual development and experimental design. Dae Bong Moon and Kyoung Song performed experiments and analyzed the data. Kyoung Song and Young Kee Shin prepared the manuscript.

References

Achord, D. T., Brot, F. E., & Sly, W. S. (1977). Inhibition of the rat clearance system for agalacto-orosomucoid by yeast mannans and by mannose. *Biochem Biophys Res Commun, 77* (1), 409-415. doi:10.1016/s0006-291x(77)80213-1

Barry, C. S., Cocinero, E. J., Carcabal, P., Gamblin, D. P., Stanca-Kaposta, E. C., Remmert, S. M., . . . Davis, B. G. (2013). 'Naked' and hydrated conformers of the conserved core pentasaccharide of N-linked glycoproteins and its building blocks. *J Am Chem Soc, 135* (45), 16895-16903. doi:10.1021/ja4056678

Becerra-Arteaga, A., & Shuler, M. L. (2007). Influence of culture medium supplementation of tobacco NT1 cell suspension cultures on the N-glycosylation of human secreted alkaline phosphatase. *Biotechnol Bioeng, 97* (6), 1585-1593. doi:10.1002/bit.21344

Borden, E. C., Sen, G. C., Uze, G., Silverman, R. H., Ransohoff, R. M., Foster, G. R., & Stark, G. R. (2007). Interferons at age 50: past, current and future impact on biomedicine. *Nat Rev Drug Discov, 6* (12), 975-990. doi:10.1038/nrd2422

Borys, M. C., Dalal, N. G., Abu-Absi, N. R., Khattak, S. F., Jing, Y., Xing, Z., & Li, Z. J. (2010). Effects of culture conditions on N-glycolylneuraminic acid (Neu5Gc) content of a recombinant fusion protein produced in CHO cells. *Biotechnol Bioeng, 105* (6), 1048-1057. doi:10.1002/bit.22644

Campbell, M. P., Royle, L., Radcliffe, C. M., Dwek, R. A., & Rudd, P. M. (2008). GlycoBase and autoGU: tools for HPLC-based glycan analysis.*Bioinformatics, 24* (9), 1214-1216. doi:10.1093/bioinformatics/btn090

Castro-Borrero, W., Graves, D., Frohman, T. C., Flores, A. B., Hardeman, P., Logan, D., . . . Frohman, E. M. (2012). Current and emerging therapies in multiple sclerosis: a systematic review. *Ther Adv Neurol Disord, 5* (4), 205-220. doi:10.1177/1756285612450936

Chen, C., Wu, N., & Watson, C. (2018). Multiple sclerosis patients who are stable on interferon therapy show better outcomes when staying on same therapy than patients who switch to another interferon.*Clinicoecon Outcomes Res, 10* , 723-730. doi:10.2147/CEOR.S163907

Diebold, M., & Derfuss, T. (2016). Immunological treatment of multiple sclerosis. *Semin Hematol, 53 Suppl 1* , S54-57. doi:10.1053/j.seminhematol.2016.04.016

Dobryszycka, W., & Kukral, J. C. (1970). Metabolic studies on sialic acid-free haptoglobin. *Arch Immunol Ther Exp (Warsz), 18* (5), 527-536.

Dumitrescu, L., Constantinescu, C. S., & Tanasescu, R. (2018). Recent developments in interferon-based therapies for multiple sclerosis.*Expert Opin Biol Ther, 18* (6), 665-680. doi:10.1080/14712598.2018.1462793

Engel, N., Weiss, V. U., Wenz, C., Rufer, A., Kratzmeier, M., Gluck, S., . . . Allmaier, G. (2015). Challenges of glycoprotein analysis by microchip capillary gel electrophoresis. *Electrophoresis, 36* (15), 1754-1758. doi:10.1002/elps.201400510

Eon-Duval, A., Broly, H., & Gleixner, R. (2012). Quality attributes of recombinant therapeutic proteins: an assessment of impact on safety and efficacy as part of a quality by design development approach.*Biotechnol Prog, 28* (3), 608-622. doi:10.1002/btpr.1548

Gasperini, C., & Ruggieri, S. (2011). Emerging oral drugs for relapsing-remitting multiple sclerosis. *Expert Opin Emerg Drugs, 16* (4), 697-712. doi:10.1517/14728214.2011.642861

Ghaderi, D., Taylor, R. E., Padler-Karavani, V., Diaz, S., & Varki, A. (2010). Implications of the presence of N-glycolylneuraminic acid in recombinant therapeutic glycoproteins. *Nat Biotechnol, 28* (8), 863-867. doi:10.1038/nbt.1651

Ghaderi, D., Zhang, M., Hurtado-Ziola, N., & Varki, A. (2012). Production platforms for biotherapeutic glycoproteins. Occurrence, impact, and challenges of non-human sialylation. *Biotechnol Genet Eng Rev, 28* , 147-175.

Goodin, D. S., Frohman, E. M., Garmany, G. P., Jr., Halper, J., Likosky, W. H., Lublin, F. D., . . . the, M. S. C. f. C. P. G. (2002). Disease modifying therapies in multiple sclerosis: report of the Therapeutics and Technology Assessment Subcommittee of the American Academy of Neurology and the MS Council for Clinical Practice Guidelines.*Neurology, 58* (2), 169-178. doi:10.1212/wnl.58.2.169

Grossberg, S. E., Oger, J., Grossberg, L. D., Gehchan, A., & Klein, J. P. (2011). Frequency and magnitude of interferon beta neutralizing antibodies in the evaluation of interferon beta immunogenicity in patients with multiple sclerosis. *J Interferon Cytokine Res, 31* (3), 337-344. doi:10.1089/jir.2010.0038

Hartung, H. P., Munschauer, F., 3rd, & Schellekens, H. (2005). Significance of neutralizing antibodies to interferon beta during treatment of multiple sclerosis: expert opinions based on the Proceedings of an International Consensus Conference. *Eur J Neurol, 12* (8), 588-601. doi:10.1111/j.1468-1331.2005.01104.x

Hokke, C. H., Bergwerff, A. A., van Dedem, G. W., van Oostrum, J., Kamerling, J. P., & Vliegenthart, J. F. (1990). Sialylated carbohydrate chains of recombinant human glycoproteins expressed in Chinese hamster ovary cells contain traces of N-glycolylneuraminic acid. *FEBS Lett, 275* (1-2), 9-14. doi:10.1016/0014-5793(90)81427-p

Hossler, P., Khattak, S. F., & Li, Z. J. (2009). Optimal and consistent protein glycosylation in mammalian cell culture. *Glycobiology, 19* (9), 936-949. doi:10.1093/glycob/cwp079

Jenkins, N., Parekh, R. B., & James, D. C. (1996). Getting the glycosylation right: implications for the biotechnology industry.*Nat Biotechnol, 14* (8), 975-981. doi:10.1038/nbt0896-975

Joosten, C. E., & Shuler, M. L. (2003). Effect of culture conditions on the degree of sialylation of a recombinant glycoprotein expressed in insect cells. *Biotechnol Prog, 19* (3), 739-749. doi:10.1021/bp0201049

Kappos, L., Freedman, M. S., Polman, C. H., Edan, G., Hartung, H. P., Miller, D. H., . . . Group, B. S. (2007). Effect of early versus delayed interferon beta-1b treatment on disability after a first clinical event suggestive of multiple sclerosis: a 3-year follow-up analysis of the BENEFIT study. *Lancet, 370* (9585), 389-397. doi:10.1016/S0140-6736(07)61194-5

Kappos, L., Polman, C. H., Freedman, M. S., Edan, G., Hartung, H. P., Miller, D. H., . . . Sandbrink, R. (2006). Treatment with interferon beta-1b delays conversion to clinically definite and McDonald MS in patients with clinically isolated syndromes. *Neurology, 67* (7), 1242-1249. doi:10.1212/01.wnl.0000237641.33768.8d

Karpusas, M., Whitty, A., Runkel, L., & Hochman, P. (1998). The structure of human interferon-beta: implications for activity.*Cell Mol Life Sci, 54* (11), 1203-1216.

Lee, S., Son, W. S., Yang, H. B., Rajasekaran, N., Kim, S. S., Hong, S., . . . Shin, Y. K. (2018). A Glycoengineered Interferon-beta Mutein (R27T) Generates Prolonged Signaling by an Altered Receptor-Binding Kinetics. *Front Pharmacol, 9* , 1568. doi:10.3389/fphar.2018.01568

Madsen, C. (2017). The innovative development in interferon beta treatments of relapsing-remitting multiple sclerosis. *Brain Behav, 7* (6), e00696. doi:10.1002/brb3.696

Mastrangeli, R., Rossi, M., Mascia, M., Palinsky, W., Datola, A., Terlizzese, M., & Bierau, H. (2015). In vitro biological characterization of IFN-beta-1a major glycoforms. *Glycobiology, 25* (1), 21-29. doi:10.1093/glycob/cwu082

Morell, A. G., Irvine, R. A., Sternlieb, I., Scheinberg, I. H., & Ashwell, G. (1968). Physical and chemical studies on ceruloplasmin. V. Metabolic studies on sialic acid-free ceruloplasmin in vivo. *J Biol Chem, 243* (1), 155-159.

Nam, J. H., Zhang, F., Ermonval, M., Linhardt, R. J., & Sharfstein, S. T. (2008). The effects of culture conditions on the glycosylation of secreted human placental alkaline phosphatase produced in Chinese hamster ovary cells. *Biotechnol Bioeng, 100* (6), 1178-1192. doi:10.1002/bit.21853

Noguchi, A., Mukuria, C. J., Suzuki, E., & Naiki, M. (1995). Immunogenicity of N-glycolylneuraminic acid-containing carbohydrate chains of recombinant human erythropoietin expressed in Chinese hamster ovary cells. *J Biochem, 117* (1), 59-62. doi:10.1093/oxfordjournals.jbchem.a124721

Royle, L., Campbell, M. P., Radcliffe, C. M., White, D. M., Harvey, D. J., Abrahams, J. L., . . . Dwek, R. A. (2008). HPLC-based analysis of serum N-glycans on a 96-well plate platform with dedicated database software. *Anal Biochem, 376* (1), 1-12. doi:10.1016/j.ab.2007.12.012

Royle, L., Radcliffe, C. M., Dwek, R. A., & Rudd, P. M. (2006). Detailed structural analysis of N-glycans released from glycoproteins in SDS-PAGE gel bands using HPLC combined with exoglycosidase array digestions. *Methods Mol Biol, 347* , 125-143. doi:10.1385/1-59745-167-3:125

Sareneva, T., Pirhonen, J., Cantell, K., & Julkunen, I. (1995). N-glycosylation of human interferon-gamma: glycans at Asn-25 are critical for protease resistance. *Biochem J, 308 (Pt 1)* , 9-14. doi:10.1042/bj3080009

Sola, R. J., & Griebenow, K. (2010). Glycosylation of therapeutic proteins: an effective strategy to optimize efficacy. *BioDrugs, 24* (1), 9-21. doi:10.2165/11530550-000000000-00000

Song, K., Yoon, I. S., Kim, N. A., Kim, D. H., Lee, J., Lee, H. J., . . . Shin, Y. K. (2014). Glycoengineering of interferon-beta 1a improves its biophysical and pharmacokinetic properties. *PLoS One, 9* (5), e96967. doi:10.1371/journal.pone.0096967

van Beers, M. M., Jiskoot, W., & Schellekens, H. (2010). On the role of aggregates in the immunogenicity of recombinant human interferon beta in patients with multiple sclerosis. *J Interferon Cytokine Res, 30* (10), 767-775. doi:10.1089/jir.2010.0086

Walsh, G., & Jefferis, R. (2006). Post-translational modifications in the context of therapeutic proteins. *Nat Biotechnol, 24* (10), 1241-1252. doi:10.1038/nbt1252

Wright, A., & Morrison, S. L. (1997). Effect of glycosylation on antibody function: implications for genetic engineering. *Trends Biotechnol, 15* (1), 26-32. doi:10.1016/S0167-7799(96)10062-7

Wurm, F. M. (2004). Production of recombinant protein therapeutics in cultivated mammalian cells. *Nat Biotechnol, 22* (11), 1393-1398. doi:10.1038/nbt1026

Zhang, S., Li, W., Lu, H., & Liu, Y. (2017). Quantification of N-glycosylation site occupancy status based on labeling/label-free strategies with LC-MS/MS. *Talanta, 170* , 509-513. doi:10.1016/j.talanta.2017.04.053

Table 1. Sialylation content and variation

Sialylation contents and variation	R27T	Rebif
Neu5Ac (mol/mol protein)	2.75	0.77
Neu5Gc (mol/mol protein)	0.06	-
Total sialic acid content (mol/mol protein)	2.81	0.77
Galactose (mol/mol protein)	10.00	2.48
Capping ratio	0.28	0.31

Table 2. Summary of average values for the relative percentage of different antennary structures

Structure	Relative percentage (%)
% A2	42.5
% A3	6.3
% A3'	10.9
% A4	8.8
% Fuc	94%
% Lac	29.3

*Please see Structure abbreviations section, Supporting Information.

Table 3. N-glycan profiles

Peak ID	WAX (whole pool)	WAX (whole pool)	R27T WAX (fractions)	R27T WAX (fractions)	R27T WAX (fract
	GU	% Area	GU	Major structure	GU
1	7.18	0.74	7.2	A2G2	
2	7.42	0.8		3	
3	7.56	2.45	7.6	FA2G2	
4	7.97	15.99	8	FA2G2S1	
5					
6	8.46	39.85	8.4	FA2G2S2	8.5
7	8.92	12.42	8.9	FA2G2S*2	
8	9.31	3.71	9.3	FA3‘G3S1	9.3
9	9.7	6.75	9.7	FA3G3S3	9.6
10	10.1	6.48	10.1	FA3‘G3S3	
11	10.55	1.56	10.6	FA3‘G3S*3	10.6
12	10.85	0.82	10.6	FA4G4S1	10.6
13	11.2	2.82	11.2	FA4G4S3	11.2
14	11.53	2.36	11.5	FA4G4S4	11.8
15	11.94	1.13	11.7	FA4G4S*3	11.7
16	12.13	0.31	11.9	FA4G4S*4	
17	12.21	0.64	12.2	FA4G4Lac1S3	12.2
18	12.45	0.86	12.4	FA4G4S*4	12.4
19	12.87	0.1	12.7	FA4G4Lac1S*3	12.7
20			12.9	FA4G4Lac1S4	12.8
21	13.35	0.19	13.2	FA4G4Lac2S3	13.2
22	>13.4		13.6	FA4G4Lac2S*3	13.6

Number of sialic acids is 0S (gray), 1S (green), 2S (blue), 3S (brown), and 4S (red).

*Please see Structure abbreviations section, Supporting Information

Figure 1.

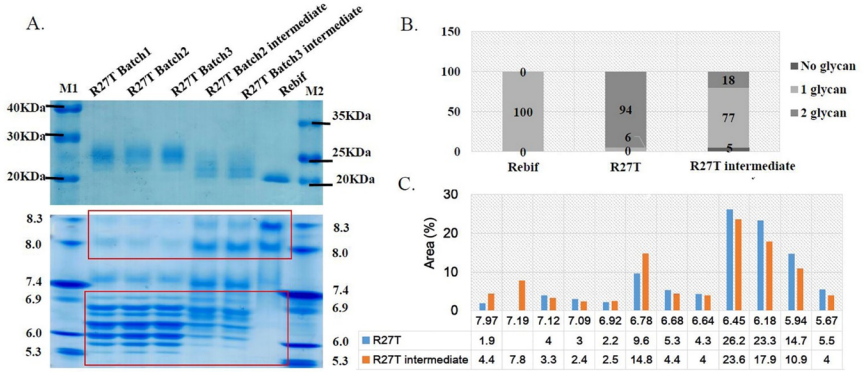

N-glycosylation site occupancy heterogeneity reflects R27T size and pI differences. (A) SDS-PAGE and IEF analysis of glycoproteins. Lanes 2-4 show the main target peaks from R27T purification, and lanes 5-6 show intermediate peaks comprising mainly non- or partially glycosylated protein. Lane 7 is the singly glycosylated Rebif reference. (B) Microchip analysis (C) cIEF analysis

Figure 2.

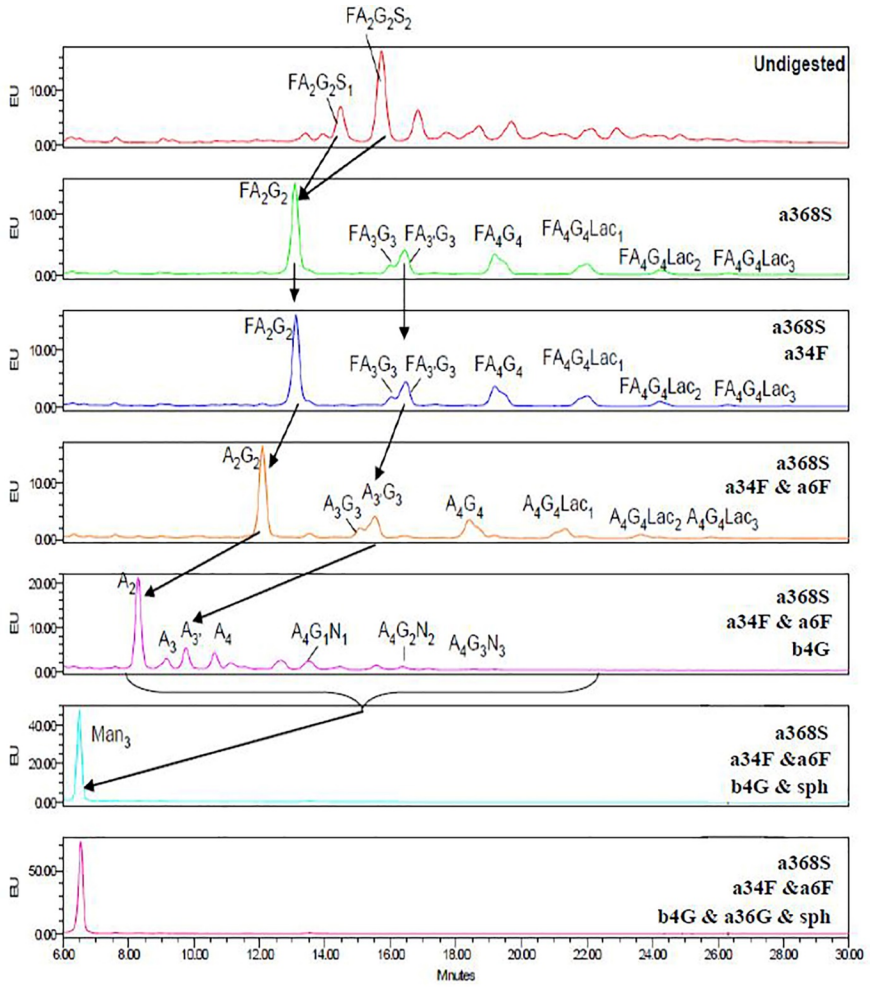

Exoglycosidase digestion sequencing of the R27T N-glycan by HILIC-HPLC Arrows indicate digestion. The following exoglycosidases were used: sialidase (a368S; specific for α2-3, -6, -8, and -9 sialic acids); beta-galactosidase (b4G; specific for β1-4 galactose); α-galactosidase (a36G; specific for α1-3/6 galactose); fucosidase (a34F; specific for α1-3 and -4 fucose); fucosidase (a6F; specific for α1-6>2 fucose); *N* -acetylglucosaminidase (sph; specific for β-GlcNAc). Glycan structures were allocated by a combination of elution position (expressed as GU value) and subsequent GU values of peaks following digestion with specific exoglycosidases. * Please see Structure abbreviations section, Supporting Information.

Figure 3.

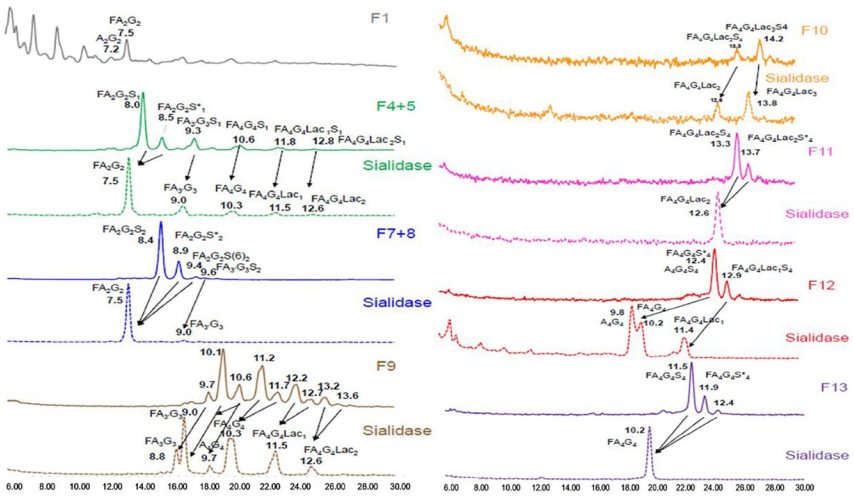

HILIC-HPLC profiles of R27T WAX fractions before and after sialidase digestion.

*Please see Structure abbreviations section, Supporting Information

Figure 4.

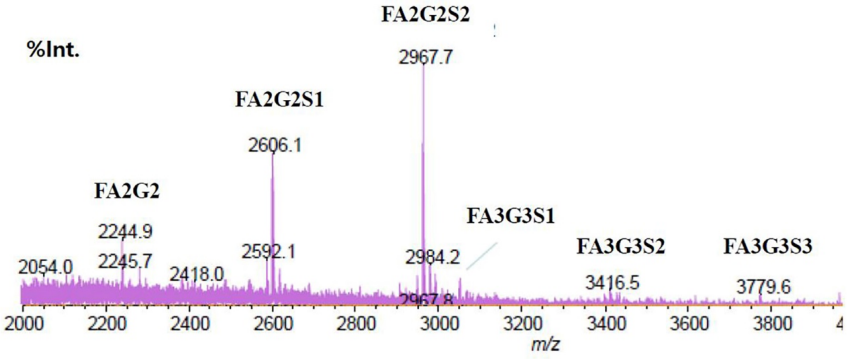

MALDI-MS spectra from permethylated R27T. m/z [M+Na]+H = hexose, N = N-acetylhexosamine, F = fucose (deoxyhexose).